EXPLICIT DYNAMIC SIMULATION OF A DUPLEX AND SUPERDUPLEX STRIP FORMING PROCESS*

Marlon Galileu Rizzo[1]
Marcelo Lucas Pereira Machado[2]

Abstract

Flexible Pipe Manufacturing Processes are increasingly being subjected to the need to improve the resilience of materials, due to the higher depth of oil exploration. Among these materials is the steel strip responsible for manufacturing the first layer of the flexible pipe, called by the carcass, which is liable for withstanding the internal pressure of the product passing through the inner of the pipe. Currently, steel strips with bigger size are being used in the Duplex material. The mechanical and microstructural characteristics were evaluated. This paper aims at modelling of a mechanical forming process of Duplex and Superduplex Stainless Steel strips through Computational Simulation Software (ANSYS LS-Dyna and ABAQUS) in order to perform explicit dynamic analyzes in which the material supports higher efforts in a short period of time. The Explicit Computational Simulation was made associated with an industrial case, obtaining a simulation compatible with the real process, being possible to validate the model. Finally, after the validation of the model, a computational analysis was done between the Duplex and Super Duplex materials, in which it was possible to detect some points of the strip with greater stresses.

Keywords: Forming; Computational simulation; Duplex; Superduplex;

[1] *Aluno de Mestrado do curso de Pós-Graduação em Engenharia Metalúrgica e de Materiais, Instituto Federal do Espírito Santo, Vitória-ES, Brasil.*

[2] *Doutor em Metalurgia e Materiais, Departamento de Metalurgia e Materiais, Instituto Federal do Espírito Santo, Vitória-ES, Brasil.*

1 INTRODUCTION

Debold [3] e Bordinassi [2] mentioned that Duplex stainless steels (AID) containing austenite and ferrite are being used in the chemical process industries and other applications where high levels of corrosion resistance and stress are required. Limit of resistance about two times compared to standard stainless steels can be obtained with localized corrosion resistance and under stresses higher than that of type 316L. In addition, Super-Duplex stainless steel alloys combines characteristics of ferritic and austenitic stainless steels in a single material and thus has higher mechanical strength and corrosion than conventional austenitic stainless steels. These steels have been used in the manufacture of flexible tube casings in different sizes of strips.
This paper aims to evaluate the stress *versus* strain curves of Duplex and Superduplex steels and to develop a computational simulation through a conceptual modeling with Ansys LS-DYNA software for the process of forming a stainless steel strip. Next, a simulation of the real process will be performed in ABAQUS software. After validating the results of the simulation process compared to the industrial process, the work aims to analyze the influence of production parameters on the properties of the material and to identify points in which the process generates the major deformations and stresses that could cause problems in the manufacturing process of the profile, and to perform a comparison of Duplex and Superduplex materials.
This work will study the forming process called profiling, in which a profiling machine is used to produce a layer of a stainless steel strip, which is profiled and interconnected (stapled) around the mandrel, called the carcass and which composes the first layer of a flexible tube applied in offshore operations.
Remita, Marchand and Taravel-condat [6] explains that the first stage of the carcass manufacturing process consists of a cold forming of a flat strip through a configuration of profiling tools to reach the specified profile. The different steps during the manufacture of the housing are shown in figure 1:

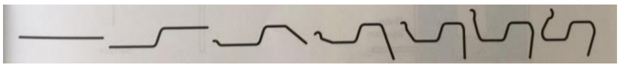

Figure 1. Stages of the Process of Profiling of a Stainless Steel Strip [6]

According to Silva and Paulo [8], Stainless steels have high Cr content in their composition, above 12%, which guarantees this material an increase of resistance to oxidation and corrosion. These steels have a great interest for engineering, due also to the two mechanical properties at high temperatures and toughness. Duplex stainless steels are typically hot worked in the range of 1000-1200 °C, in a region of $\alpha + \gamma$ phases, and temperatures above this range may cause oxidation problems and below it may result in precipitation associated with embrittlement. Ferritic-austenitic Duplex stainless steels have microstructures consisting of approximately equal fractions of these two phases, as shown in the figure 2.

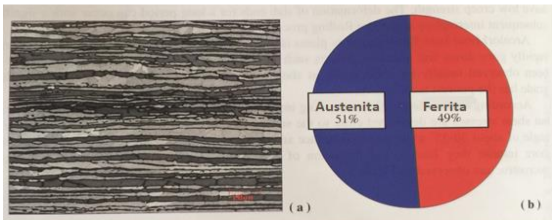

Figure 2. Microstructure and Phase of a Strip with 5.00 mm Thickness and Grade 2205

These steels are characterized by a favorable combination of the properties of ferritic (γ) and austenitic (α) stainless steels: it has high mechanical strength, good toughness, resistance to stress corrosion and fatigue. This microstructure and combination of properties are generally obtained by increasing the chromium and molybdenum contents in relation to austenitic steels and increasing the nitrogen content as an interstitial solute has a very favorable effect on the mechanical strength. These changes in chemical composition increase the stability of the sigma phase and allow the appearance of some other intermetallic phases, especially the phase chi (χ) flame, Fe30Cr18Mo4. The designation Superduplex is related to the equivalent number of corrosion resistance (PREN) and Critical Corrosion Temperature (CPT), as shown by Zuili [9] and Pinto [4]. CPT can be obtained by a test using ASTM G48 or ASTM G150. PREN is obtained by the equivalent amounts of the following components: % Cr + 3.3 x% Mo + 16 x% N. From the PREN formula it is possible to notice that the larger quantities of the Cr, Mo and N elements, the higher PREN value, which can be observed in Table 1, that shows the PREN and CPT differences between Duplex and Superduplex:

Table 1. PREN e CPT do Duplex 2205 e do Superduplex 2507 [4 e 9]

DUPLEX STAINLESS STEEL	COMPOSIÇÃO	PREN	CPT (ºC)
Duplex 2304	23%Cr-4%Ni-0,10%N	26	22 - 28
Duplex 2205	22%Cr-5%Ni-3%Mo-0,17%N	34 – 38	30 – 35
Superduplex 2507	25%Cr-6,8%Ni-3,7%Mo-0,27%N	38 - 47	45 – 65

Three different types of Duplex steels are studied in this work:

- Duplex stainless steel strip: NF EN 10088-2 grade 1.4462 UNS S 31803;
- Duplex stainless steel strip: NF EN 10088-2 grade 1.4362 UNS S 32304;
- Superduplex stainless steel strip: NF EN 10088-2 grade 1.4410 UNS S 32750.

ROMMERSKIRCHEN, SCHÜLLER, SOELCH, et al., described in the table 2, the Chemical Composition of the different grids of Stainless Steel Duplex:

Table 2. Chemical Composition of the different grids of Stainless Steel Duplex [7]

Grade	%C	%Mn	%Cr	%Ni	%Mo	%N	%Si	%P	%Cu	%S
1.4462	≤ 0.03	≤ 2.00	21 - 23	4.5 - 6.5	2.5 - 3.5	0.10 - 0.22	-	-	-	-
1.4362	≤ 0.03	≤ 2.00	23.0	4.4	0.25	0.11	≤ 1.00	≤ 0.03	0.25	≤ 0.02
1.4410	≤ 0.03	≤ 2.00	24 - 26	6.0 - 8.0	3.0 - 4.5	0.24 - 0.35	-	-	-	-

SILVA and PAULO [8], present in table 3 the comparison of the mechanical properties between the main stainless steels:

Table 3. Mechanical Properties of Main Stainless Steels [8]

Type		Austenitic	Ferritic	Duplex		
Grade		S 30400	S 43000	S 32304	S 31803	S 32750
Ultimate tensile strength	**MN/m²**	515-690	450	600-820	680-880	800-1000
Yield Strength	**MN/m²**	210	205	400	450	550
Elongation	**%**	45	20	25	25	25
Energy Absorbed in Charpy V Test at ºC amb.	**J**	> 300	-	300	250	230
Fatigue strength	**MN/m²**	120 ± 120	-	245 ± 245	285 ± 285	300 ± 300

The typical stress-strain curve obtained from tensile tests was performed by ARRAYAGO, REAL and GARDNER [1] and is shown in figure 3:

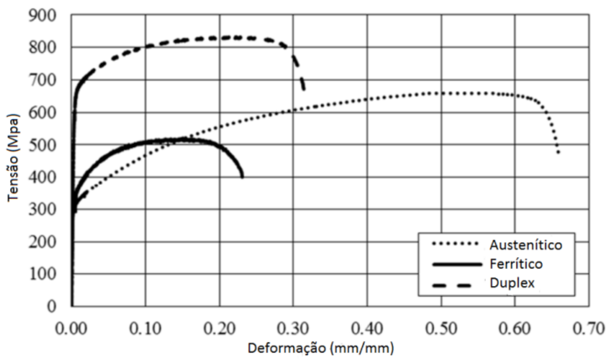

Figure 3. Stress *versus* Strain curve of Austenitic, Ferritic and Duplex Steels [1]

2 MATERIAL AND METHODS

2.1 Samples for Tensile Test

The materials used for this paper were Duplex stainless steels of two types: Duplex NF EN 10088-2, grade 1.4362 - UNS S32304 and Superduplex NF EM 10088-2 grade 1.4410 UNS S 32750.

To ensure the simulation of the current material and to obtain the stress *versus* strain curve data, several specimens were from 1.8 mm and 2.6 mm thick sheet metal for the Duplex material and with 3.00 mm of thickness for the Superduplex material, as shown in figure 4:

Figure 4. Samples of a Duplex Rolled Steel

The microstructure of the material was evaluated through the laboratory micrograph of the laminated strip of Duplex and Superduplex steels, according to figure 5:

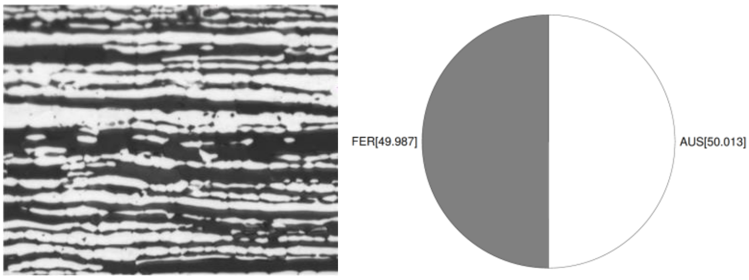

Figure 5. Microstructural Analysis of Duplex Samples

For the material Superduplex NF EN 10088-2, grade 1.4410 - UNS S32750, two specimens of 3 mm thickness were obtained, the first one in the longitudinal direction and the another one in the transversal direction of rolling process. The material has Poisson Coefficient 0.3 and specific gravity of 7.8 kg/dm³. The microstructural analysis of the supplier indicates that the material contains 49% ferrite.

2.2 Conceptual model of the profiling process

Because the profiling process consists of many variables, a high rate of deformation over time and also with variables such as speed and rotation, the first need was to use software that would allow us to create an explicit simulation.
The input data for the conceptual simulation were:
a) Initial strip velocity: 8,000 mm / s. This speed is much higher compared to current production due to the processing time it would take to calculate. Since for the conceptual model, the solution would not yet be validated with the real profile, it was decided to extend the race time, thus reducing the simulation time.
b) Rotation speed of the rollers: 1200 rpm. As well as speed, the rotation of the discs has also been increased to reduce the simulation time.
c) For the conceptual analysis, a standard steel of the software library was chosen for the disks and the main guide, with a linear elastic formulation, as given below:

- E = 193 Gpa
- Poisson = 0.31

d) For the conceptual analysis, a standard steel of the software library, with an isotropic bilinear formulation, was chosen for the strip, as given below:

- E = 193 Gpa
- Poisson = 0.31
- σ_y = 210 MPa
- Tangent Modulus = 1,8 GPa

The geometry is initially made in 2D format and then passed to the 3D format, as shown in figure 6:

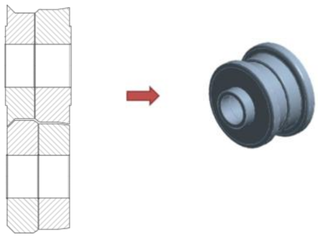

Figure 6. 3D modeling of profile rollers

The faces of the disk were divided into 4 parts, in order to facilitate the generation of mesh in these bodies, as shown in the figure 7:

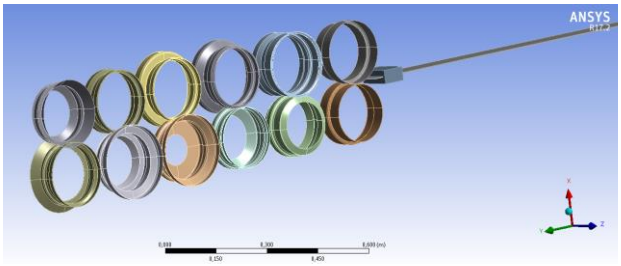

Figure 7. Geometry in Shell Model for Mesh Processing in Ansys Software

For the strip, the thickness was divided into 6 elements through the Sweep method, and for the rollers, meshes of the Multizone Quad / tri method type were generated, as shown in the figure 8:

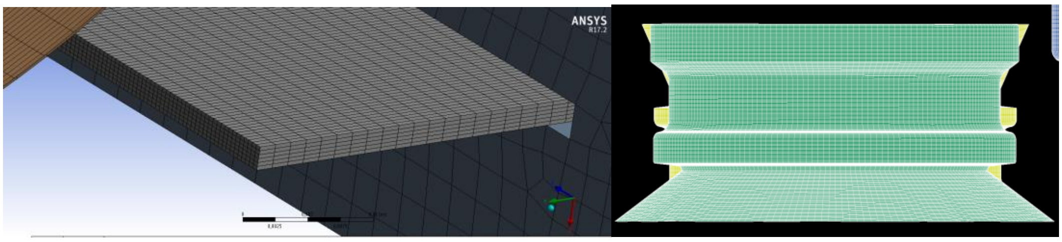

Figure 8. Mesh generated in the Geometry of Duplex Stainless Steel strip and the Rollers

The contact between each roller and the strip was a Frictional type, being the target the own disc. A dynamic coefficient of friction of 0.2 with an asymmetric behavior was used. Between the strip and the guide was defined a contact of the type Frictionless, being the target the guide.
For all the rollers the condition Rigid Body Contraint was inserted, being fixed in the X and Y axes, and free for rotation in the Z axis. For the guide the Rigid Body Contraint condition was inserted, being fixed in all directions, without possibility of rotation in any axis. Still for the rollers, the Rigid Body Angular Velocity contour condition was created to allow rotation of the discs only on the X axis and to set the angular velocity value.

3 RESULTS AND DISCUSSION

3.1 Post-processing - Conceptual Model analysis

The analysis of the results shows which regions had the highest plastic strains. It can be observed in the figure 9, that the regions in which they presented the highest values of stress, and consequently they had the greatest deformations, was the central region of the strip forming, and the lateral regions, being this only when the process begins the forming of the ends of the strip.

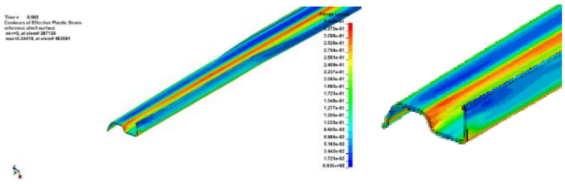

Figure 9. Post-processing analysis of the Model

For the analysis of the conceptual model, the objective was to verify if the simulated profile was similar to the theoretical profile. A cross section was performed in the simulated profile as shown in the figure 10.

Figure 10. Cross Section on the 3ª Profiling Operation

* Technical contribution to the 74º Congresso Anual da ABM – Internacional, part of the ABM Week 2019, October 1st-3rd, 2019, São Paulo, SP, Brazil.

In figure 11 it can be observed that the simulated profile was able to obtain the dimensions close to the theoretical profile.

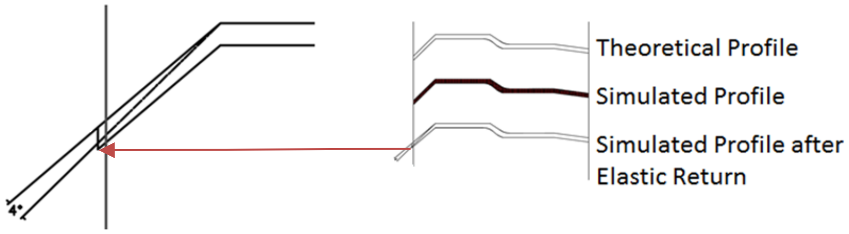

Figure 11. Simulation of the Elastic Return after the 3rd Profiling Operation

Although the conceptual model has a positive tendency to reproduce the profiling process through a computational simulation, it was possible to find points that hinder the computational process, among them:

- Large plastic strain;
- Tendency of elastic return of material between steps;
- Time of the process too long for an explicit analysis;
- Contact configuration: tendency of bodies to penetrate.

3.2 Tensile Test and data analysis

From the data obtained from the tensile test on the Duplex rolled steel, it was possible to obtain the strain x strain curve by plotting the result of all the samples, as shown in figure 12:

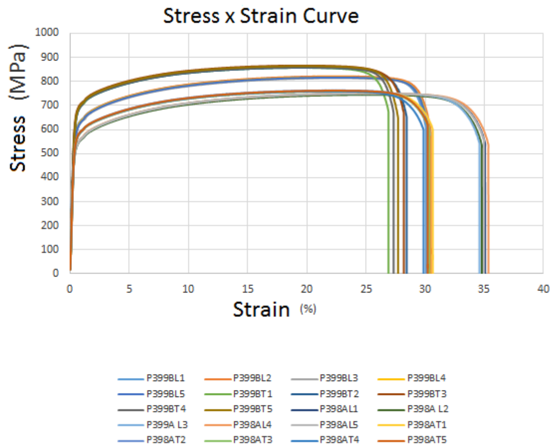

Figure 12. Stress *versus* Strain curve of Duplex Samples

The data of figure 12 were treated separately to create a curve considering 5 distinct cases, including the true stress and strain, as shown in the graph of figure 13:

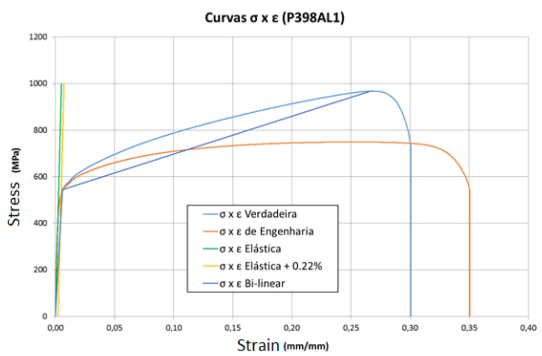

Figure 13. True Stress *versus* Strain curve of Duplex Samples

The graph of figure 13 shows coherence of the values of maximum tensile stress with the stress *versus* strain curve shown in figure 3 and in table 3, with values between 800 and 1000 ° C. Moreover, in the true stress *versus* strain curve of the graph of figure 14, the yield limit values are compatible with those shown in table 3, with values between 400 and 600 MPa.
The graphs plotted from the stress *versus* strain curve of the tensile tests performed with the Superduplex test samples is shown in the figure 14:

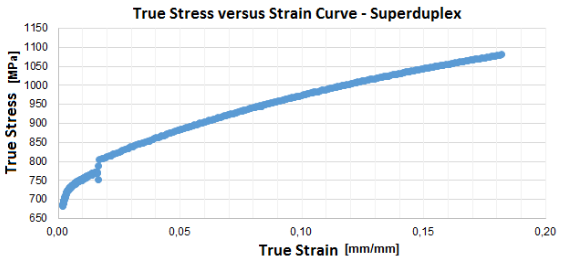

Figure 14. True Stress *versus* Strain curve of Superduplex Samples

The results of the tensile tests show that the Superduplex has tensile strength values that can exceed values of 1000 MPa, showing a higher mechanical resistance compared to Duplex.

3.3 Microstructural analysis of materials

In order to evaluate if there were other phases besides ferrite and austenite in the materials being evaluated, two different samples of Duplex and Superduplex were characterized and evaluated according to their microstructure. The profile used was the final profile of the profiling process. The areas evaluated were as shown in figure 15:

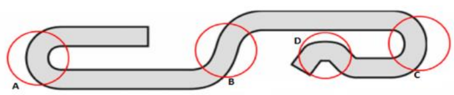

Figure 15. Profile Areas for Micrographic Analysis

The results of the micrographic analysis of the profile for the Duplex and Superduplex are presented in figure 16,

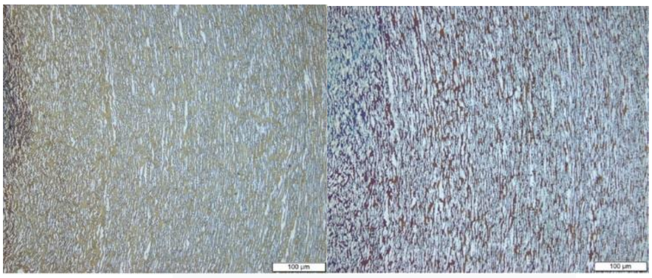

(a) (b)

Figure 16. Microscopic Analysis of Duplex Steel Profile (a) and Superduplex Steel Profile (b)

The results showed coherent values of ferrite in the microstructure, as shown in the table 4 and being verified in figure 2.

Table 4. % Ferrita by regions of the sample of Duplex and Superduplex (1000x)

	MEASUREMENTS REGIONS OF FERRITE (%)			
REGIONS	**A**	**B**	**C**	**D**
SUPERDUPLEX	46,75	48,75	51,35	46,94
DUPLEX	51,48	49,66	50,63	49,23

However, for the Superduplex, the presence of the sigma phase was also observed, as shown in figure 17.

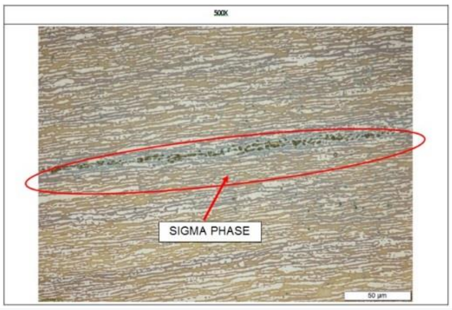

Figure 17. Presence of the Sigma phase in the Superduplex Steel profile

3.4 Real Computational Simulation

From the results obtained with the conceptual model in which it was possible to simulate the strip forming process (profilling), a new simulation was made, already considering all the real data of the industrial process. For the real model, there was a change in the strip dimensions, considering a profiling process with 10 steps.
Due to the high degree of strain that the stainless steel strip undergoes during the profiling process and due to the fact that these deformations occurred in a very short time, in order to guarantee more agility to the processing, the same simulation methodology was used in the Abaqus software, in which at the time of execution of this work, there was a greater availability of processors and licenses.
Due to the large deformations suffered by the strip in a short period of time, the ABAQUS software module chosen to perform the simulation was ABAQUS/Explicit.
The profile rollers are made of standard steel, quenched and tempered ensuring enough strength to be non-deformable and with high resistance to wear. These are free of rotation about their axis and the minimum distance between each roller of each operation is 2.7 mm, with a negative variation of 0.03 to 0.08 mm caused by the tightening of the rollers, thus allowing a variation of not more than 2,96% of the nominal thickness. Between each operation of the profiling rollers the distance is 210 mm. In the same way that was considered for the conceptual model, the geometry of the rolls was defined in the shell format, with a thickness of 1 mm towards the center of the roller.
The geometry was created in the Inventor Software, from the import of 2D models in .dwg format. Then the geometry in .stp format was imported into ABAQUS.
In this new simulation, the main guide was not inserted, in order to see if without this support there would be deviations in the simulation.
From the mechanical properties obtained in item 3.2, the strip material was considered isotropic elastoplastic. The strip was considered to be a homogeneous solid and the main input properties in the software were inserted as elastic, plastic and density properties as well as the data of the true stress *versus* strain curve of the material, according to the information indicated in item 3.2. Initially, the *current* model

was made with the material data of the Duplex stainless steel strip and then with that of the Superduplex material.
As for the rollers, the geometry was defined as a rigid 3D discrete body, and it is not necessary to include material data, since this body will not suffer deformations.
The methods used for the mesh were the same indicated in the conceptual simulation shown in the item 2.2. The results for the strip and for the rollers are indicated in the figure 18.

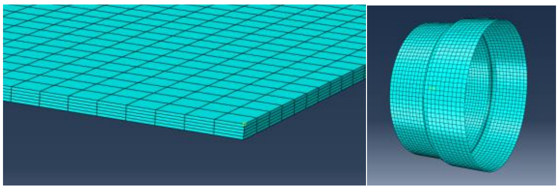

Figure 18. Strip and Rollers Meshes

The contact conditions between the various faces of the geometries were defined as being of surface-to-surface type, as shown in figure 19.

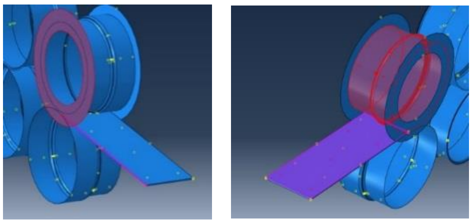

Figure 19. Contact type of surface-to-surface

The main conditions considered in the simulation are described below:

- The speed of rotation of the rollers was defined in radians/second, based on the speed of production with the value of 5.97 rad/s;
- The strip speed was defined as the linear velocity pattern that this strip passes through the profiling operations with a value of -15.4 m/min;
- An initial velocity applied to the front of the strip (last to enter the rollers) was also defined, in order to represent the beginning of the profiling process, since the simulation does not present a constant forming process with a value of -30 m/min;
- A Mass Scaling condition was also applied with an increase of 1e-6.

In order to validate the model, the geometry of the theoretical profile was compared to the geometries of a real sample taken after the seventh operation (see figure 21) of the profiling process and with another sample taken from the computational simulation at the same stage. The three profiles are shown in the figures 20.

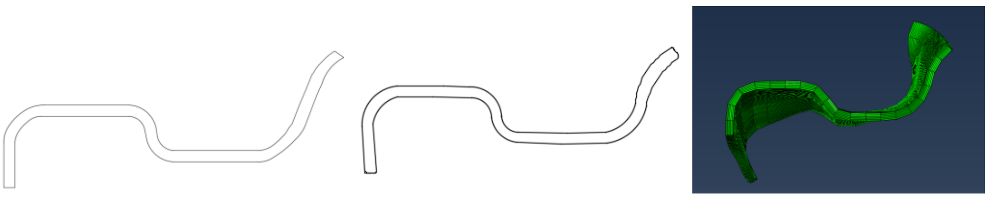

(a) (b) (c)

Figure 20. Theoretical profile (a), Real profile (b) and Simulated profile (c) after seventh step of profiling process

(a) (b)

Figure 21. Samples removed after seventh step of profiling process (a) and Measurements regions (b)

The profiles were evaluated in the Autocad Software, performing measurements to compare the regions indicated in the figure 21-b.
The results of the measurements are shown in the table 5:

Table 5. Comparison of measurements between theoretical, real and simulated profiles

Profiles	A	B	C	D	E
Nominal Thickness of the Strip	2,7	2,7	2,7	2,7	2,7
Real Sample	2,68	2,66	2,7	2,65	2,71
Simulated Profile	2,65	2,64	2,63	2,63	2,65
Variation between Real Sample and nominal thickness	0,70%	1,50%	0,00%	1,90%	-0,40 %
Variation between Simulated profile and nominal thickness	1,90%	2,20%	2,60%	2,60%	1,90%
Variation between the Real Sample and Simulated Profile	1,10%	0,80%	2,60%	0,80%	2,20%

From the values measured in table 5, the average difference of the thicknesses found of the simulated profile compared to the real profile has a difference measurement of 1.5%. This result presents a very good level of the simulation, considering that the maximum value of variation is 2.66% for the tolerances of the thicknesses, and the both results are below of the 2,96% indicated in the item 3.4.

3.5 Analysis of software parameters and results

Simulation of the profiling process with real strip data showed some regions where the strip undergoes greater stresses and thus has higher stress. In the computational simulation of the Duplex Stainless Steel Strip profiling process, it was possible to identify points after the seventh profiling operation with high stress values, it may be possible to obtain points of failure when subjected to stresses of the carcass during offshore operation, as shown in Figure 22.

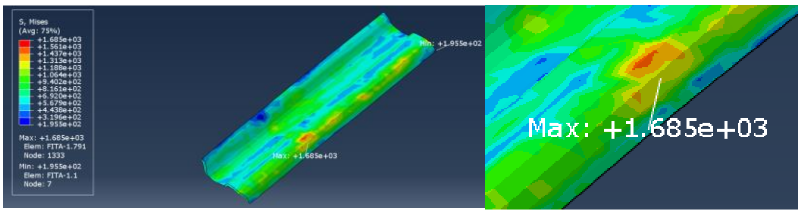

Figure 22. Voltage Result on Stainless Steel Duplex Strip after the seventh profiling operation

In the figure 23, it can be possible identify regions where there are higher stresses in the Superduplex steel strip.

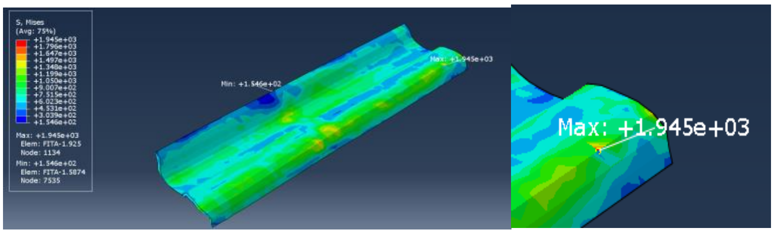

Figure 23. Results of the strip stresses throughout the operations until the seventh profiling operation

For both materials no excessive points of plastic deformation were found throughout the process, as shown in the figure 24, except for a single region at the end of the strip, which could be solved by a better refinement of the mesh at that point.

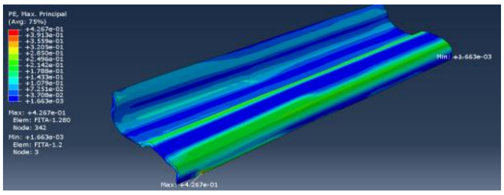

Figure 24. Plastic Strain on Duplex and Super Duplex Stainless Steel Strips

4 CONCLUSION

The computational tools used by the software Ansys-LS-Dyna and ABAQUS/Explicit based on dynamic explicit modeling method, in order to automate the industrial profiling process, and thus obtain results like stress, deformation, springback angle, among other properties, had stable results of the forming process and in the two softwares the results of the simulated profiles compared to the real profiles were similar, with small variations.
Regarding to the materials analysis, the stress *versus* strain curves of the materials showed consistent values between the theoretical data of these materials, and the micrographic analysis found that the microstructure of the materials evaluated is compatible with the Duplex and Superduplex Steels. However, the presence of sigma phase was observed in the Superduplex Steel, which can give this material a brittleness and lower mechanical resistance.
It was observed the maximum levels of accumulated plastic deformations were detected in region A after the seventh stripping operation. And the highest levels of stress are observed in modeling operations on the main surface of the strip which the largest value observed was around of 1500 MPa, indicating the necessity of improvements to be made in forming tooling to reduce loads and efforts in the regions with higher stresses.
It was highlighted during the discussions that despite the results of the stress suffered by the material in this work show a more satisfactory result for Superduplex, phase sigma present in this material may weakens it and reduce its toughness, requiring advanced studies before choosing this material for application.

REFERENCES

1 Arrayago I.; Real E.; Gardner L. Description of stress-strain curves for stainless steel alloys. Materials and Design. 2015. p.540-552.

2 Bordinassi, Éd Claudio; Stipkovic Filho, Marco; Batalha, Gilmar Ferreira; Delijaicov, Sergio; Lima, Nelson Batista de. Study of residual stress in a super Duplex stainless steel after turning. Anais. Águas de São Pedro: ABCM, 2007.

3 Debold T. A. Duplex Stainless Steel – Microstructure and Properties, J. Metals: Bangkok. 1989. v.41, n.3, p 12-15.
4 Pinto B. T. Comportamento mecânico de um aço inoxidável Duplex do tipo 2205 sob a influência da temperatura e da precipitação de fases frágeis. Unicamp: Campinas. São Paulo. 2002. P. 69-71.
5 Reick, W.; Pohl, M.; Padilha, A. F. O desenvolvimento dos aços inoxidáveis ferríticos-austeníticos com microestrutura Duplex. In: Congresso Anual Da Associação Brasileira De Metais, 47. 1992, Belo Horizonte. ABM: São Paulo.
6 Remita E.; Marchand D.; Taravel-Condat C. Qualification and Industrialization of Superduplex and Alloy 31 carcasses for unbonded flexible pipe applications, Duplex stainless steels - Conference Proceedings, BEAUNE, France. 2010. p. 603 – 612.
7 Rommerskirchen I.; Schüller T.; Soelch R.; et al. Duplex Stainless Steels in the pipe production – a historical review – new findings from exotic material to commodity. Germany, 2010.
8 Silva. C. V. L; Paulo R. M. Aços e Ligas Especiais. Editora Edgard Blücher: São Paulo. 2016. 2 ed., p. 443 – 446.
9 Zuili D. The use of Duplex stainless steels in Oil & Gas Industry - Duplex stainless steels - Conference Proceedings, BEAUNE, France. 2010. p. 576 – 582.